

## Electronic Supplementary Information

### Anion-Exchange Synthesis of Nanoporous FeP Nanosheets as Electrocatalysts for Hydrogen Evolution Reaction

You Xu, Rui Wu, Jingfang Zhang, Yanmei Shi, and Bin Zhang\*

Department of Chemistry, School of Science, Tianjin University, Tianjin 300072, P. R. China

E-mail: bzhang@tju.edu.cn

## Experimental Details

### 1. Material Synthesis.

**1.1 Chemicals:** All chemicals are analytical grade and used as received without further purification.

#### 1.2.1 Synthesis of inorganic-organic hybrid $\text{Fe}_{18}\text{S}_{25}$ -TETAH nanosheets:

$\text{Fe}_{18}\text{S}_{25}$ -TETAH nanosheets were prepared according to the reported reference with small modified procedures to obtain the sheet-like nanostructures (*Chem. Mater.* **2008**, *20*, 4749-4755). In a typical synthesis procedure, 1 mmol  $\text{FeSO}_4 \cdot 7\text{H}_2\text{O}$  and 2 mmol thioacetamide ( $\text{C}_2\text{H}_5\text{NS}$ ) were added into a mixed solvent of TETA and  $\text{H}_2\text{O}$  (total 18 mL,  $V_{\text{TETA}}:V_{\text{H}_2\text{O}} = 2:1$ ) with stirring. The mixed solution was then transferred into a 50 mL Teflon-lined stainless-steel autoclave and kept at 140 °C for 24 h and cooled down naturally. The black floccule formed after the reaction was washed by distilled water and absolute ethanol, respectively, and dried in a vacuum oven at 60 °C for 6 h.

**1.2.2 Conversion of  $\text{Fe}_{18}\text{S}_{25}$ -TETAH hybrid nanosheets into nanoporous FeP nanosheets.** For a typical synthesis, 10 mg of the free-flowing dry  $\text{Fe}_{18}\text{S}_{25}$ -TETAH precursors were then dispersed in 10 mL 1-octadecene by sonication and then placed in a 3-neck apparatus sealed using a condenser with an air-flow adapter on top. The

3-neck apparatus was then degassed under vacuum at 100 °C for about 10 min, and then heated to 280 °C under argon. TOP was injected into the above system, and then the temperature was raised to 320 °C and left at that temperature for 5 h. The reaction was then allowed to cool to room temperature. The black precipitate was then quenched with an equal volume of hexanes and centrifuged for 10 min at 12,000 rpm. The supernatant was decanted and the product was washed three times with ethanol, hexanes, and dichloromethane, respectively, dried in a vacuum oven at 60 °C for 6 h.

### **1.2.3 Synthesis of inorganic-organic hybrid CoSe<sub>2</sub>-DETA nanosheets:**

CoSe<sub>2</sub>-DETA nanosheets were prepared according to the reported reference (*J. Am. Chem. Soc.* **2009**, *131*, 7486-7487). In short, 0.5 mmol Co(AC)<sub>2</sub>.H<sub>2</sub>O and 0.5 mmol Na<sub>2</sub>SeO<sub>3</sub> were added into a mixed solution (20 ml) with a volume ratio of V<sub>DETA</sub>/V<sub>H2O</sub> = 2:1 with stirring for half an hour. The mixed solution was then transferred into a 50 mL Teflon-lined stainless-steel autoclave and kept at 180 °C for 16 h and cooled down naturally. The black floccules formed after the reaction was washed by distilled water and absolute ethanol, respectively, and dried in a vacuum oven at 60 °C for 6 h.

### **1.2.4 Conversion of CoSe<sub>2</sub>-DETA hybrid nanosheets into porous cobalt phosphide nanosheets.**

The procedure for the preparation of porous cobalt phosphide nanosheets is the same as that described in Section 1.2.2 except that the Fe<sub>18</sub>S<sub>25</sub>-TETAH nanosheets were replaced by the CoSe<sub>2</sub>-DETA nanosheets. And the temperature was raised to 350 °C and left at that temperature for 6 h.

**2. Electrochemical measurements.** All electrochemical measurements were performed using an electrochemical workstation (CHI 660D, CH Instruments, Austin, TX). Pt wire and saturated calomel electrode (SCE) were used as counter and reference electrodes, respectively. A glass carbon electrode decorated with catalyst samples were used as the working electrode. For a typical making procedure for the working electrode, 2 mg of catalyst samples were dispersed in 1mL of 5 : 1 v/v water-isopropanol mixed solvent with 10 µL 5 wt% Nafion solution, then the mixture

was ultrasonicated for at least 30 min to generate a homogeneous ink. Then 10  $\mu$ L of the catalyst ink (containing about 20  $\mu$ g of catalysts) was loaded onto a glassy carbon electrode of 3 mm in diameter (loading  $\sim$  0.28 mg/cm<sup>2</sup>). Before the electrochemical measurement, the electrolyte (0.5 M H<sub>2</sub>SO<sub>4</sub>) was degassed by bubbling argon for 30 min. The polarization curves were obtained by sweeping the potential from -0.7 to -0.2 V vs. SCE at room temperature, with a sweep rate of 2 mV s<sup>-1</sup>. The polarization curves were re-plotted as overpotential ( $\eta$ ) versus log current (log  $j$ ) to get Tafel plots for quantification of the HER activities of investigated catalysts. By fitting the linear portion of the Tafel plots to the Tafel equation ( $\eta = b \log(j) + a$ ), the Tafel slope (b) can be obtained. AC impedance measurements were carried out in the same configuration at  $\eta = 0.14$  V from  $10^5$  – 0.02 Hz with an AC voltage of 5 mV. The SCE electrode was calibrated with respect to reversible hydrogen electrode (RHE). All the potentials reported in our manuscript are against RHE.

**3. Characterizations.** The scanning electron microscopy (SEM) images and Energy-dispersive X-ray spectroscopic (EDX) analysis were taken with a Hitachi S-4800 scanning electron microscope (SEM, 5 kV) equipped with the Thermo Scientific energy-dispersion X-ray fluorescence analyzer. Transmission electron microscopy (TEM) and higher-resolution transmission electron microscopy (HRTEM) images were obtained with JEOL-2100F system equipped with EDAX Genesis XM2. Scanning TEM (STEM) elemental distributions mapping were prepared with JEOL-2100F system equipped with EDAX Genesis XM2. Specimens for TEM and HRTEM measurements were prepared via dropcasting a droplet of ethanol suspension onto a copper grid, coated with a thin layer of amorphous carbon film, and allowed to dry in air. The X-ray diffraction patterns (XRD) of the products were recorded with Bruker D8 Focus Diffraction System using a Cu K $\alpha$  source ( $\lambda = 0.154178$  nm). FTIR spectra were recorded on a MAGNA-IR 750 (Nicolet Instrument Co) FTIR spectrometer.

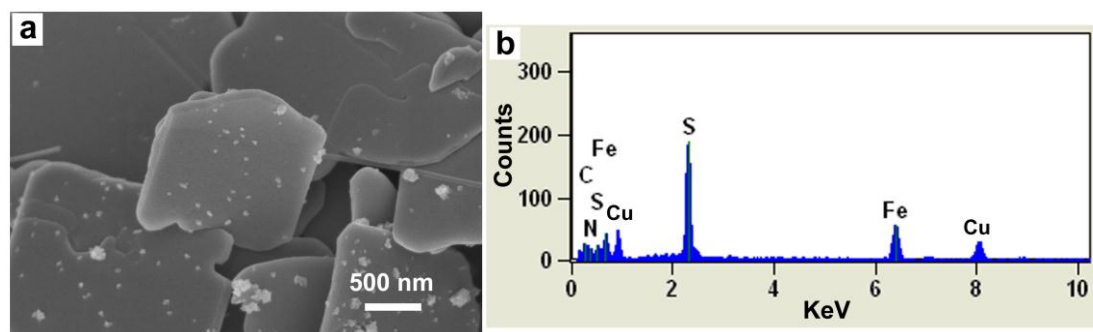


**Fig. S1** (a) SEM image and (b) EDX spectrum of the  $\text{Fe}_{18}\text{S}_{25}$ -TETAH nanosheets. In the EDX spectrum, the detected Cu singles arise from the Cu foil on which the samples were deposited.

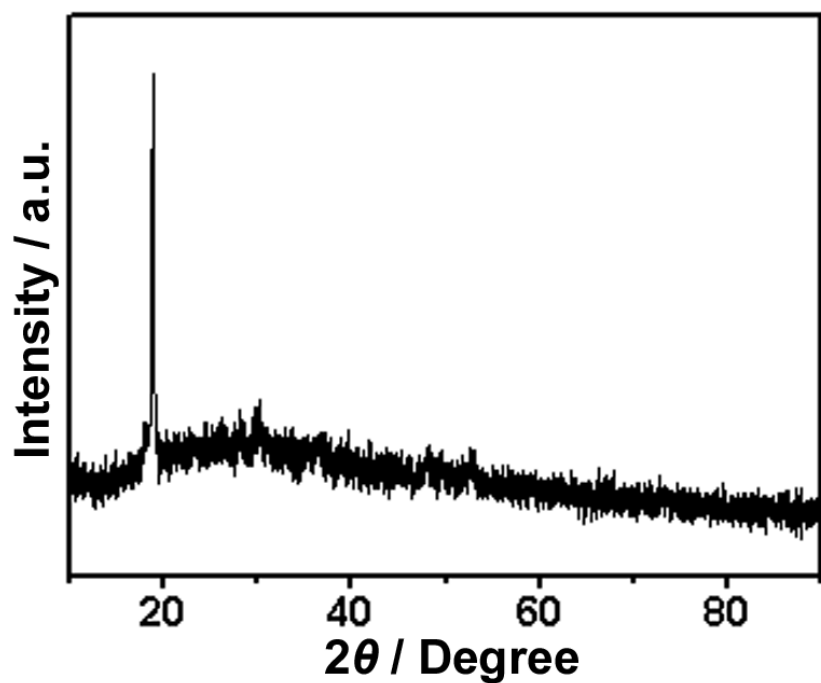


**Fig. S2** XRD pattern of the  $\text{Fe}_{18}\text{S}_{25}$ -TETAH nanosheets.

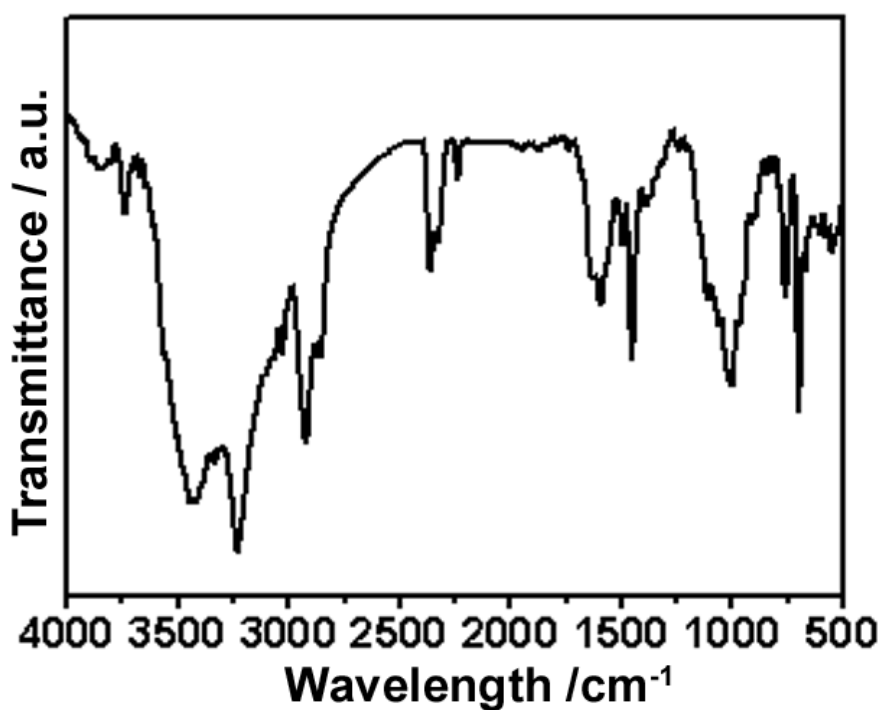


**Fig. S3** FTIR spectrum of the  $\text{Fe}_{18}\text{S}_{25}$ -TETAH nanosheets. These results (Figs. S1-3) suggest that inorganic-organic hybrid  $\text{Fe}_{18}\text{S}_{25}$ -TETAH nanosheets were prepared by using the modified amine-assisted hydrothermal method.

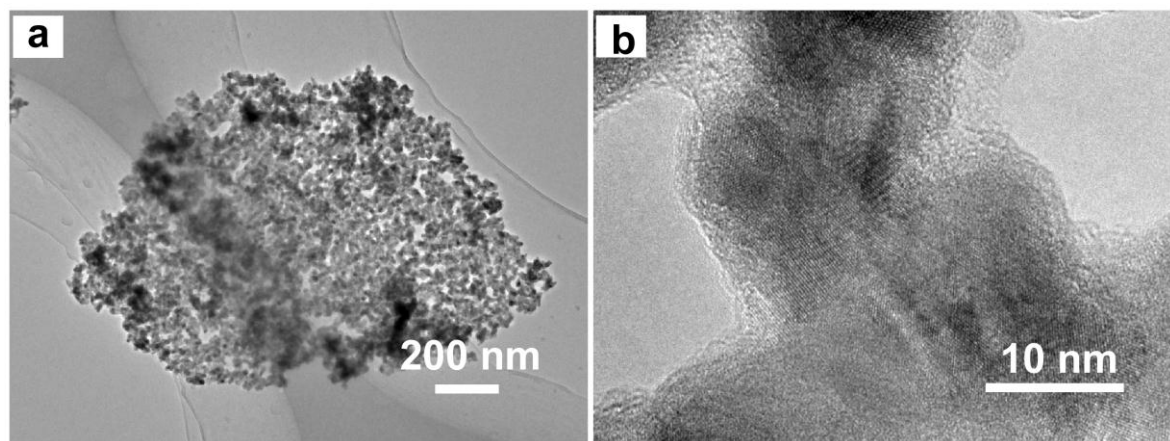


**Fig. S4** (a) TEM image of an individual porous FeP nanosheet. (b) HRTEM image of a part of the porous FeP nanosheet. It was found that the obtained products possess a 2D nanoporous sheet-like morphology and the pores distributed in the porous sheet-like products possess a wide pore size distribution rang from 5 to 50 nm.

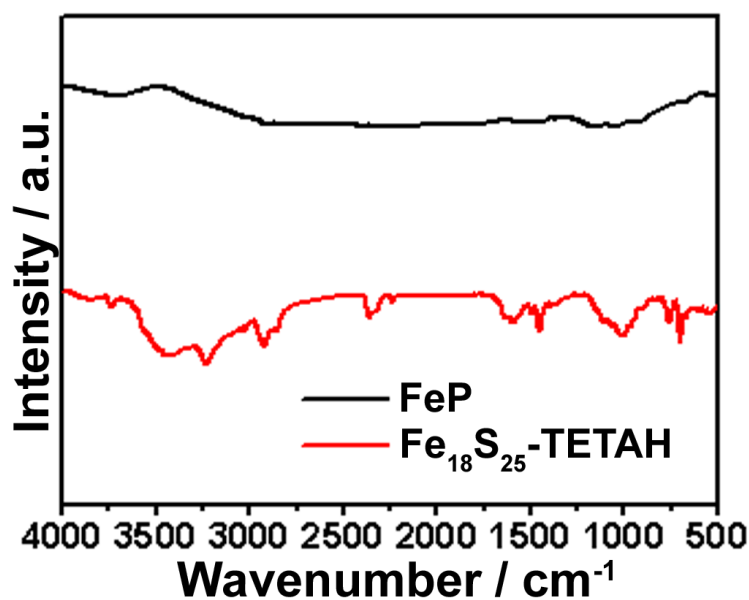


**Fig. S5** FTIR spectra of hybrid precursors and nanoporous FeP nanosheets. It was found that the absorption peaks originating from the organic molecules can not be seen in the produced porous FeP nanosheets, indicating that the hybrid precursors can be successfully transformed into inorganic materials.

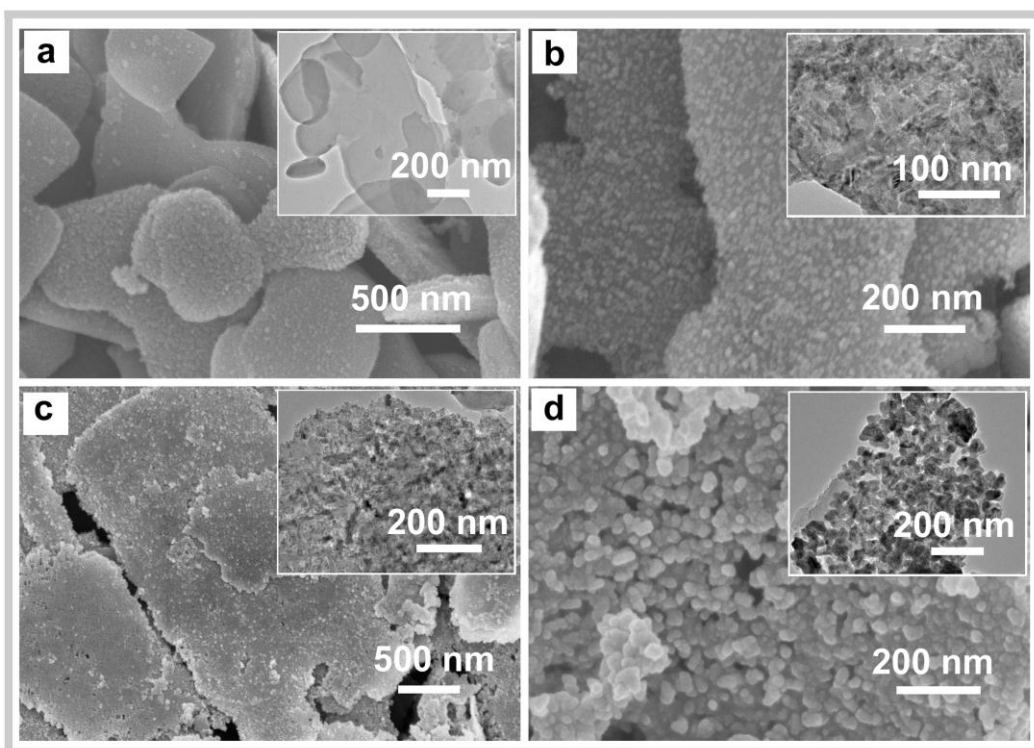


**Fig. S6** (a-d) SEM images and TEM images (the insets of a-d) of the intermediates collected at different reaction times: (a) 2 h; (b) 3 h; (c) 4 h; (d) 5 h. It can be seen that the intermediates retain two-dimensional macro-sized morphology defined by the starting precursors with the gradual appearance of nanopores throughout the nanosheets.

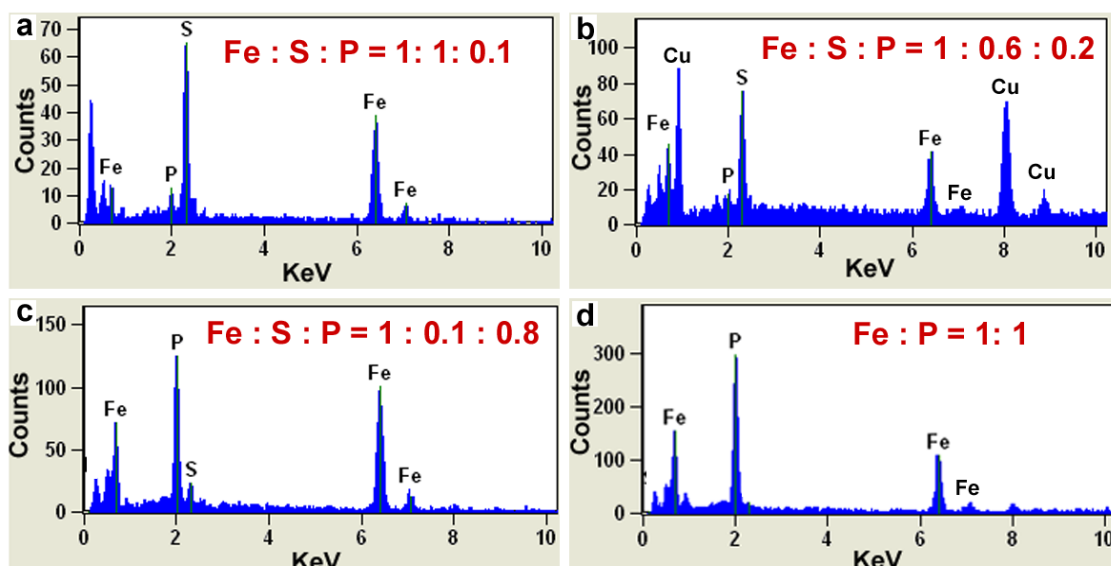


**Fig. S7** EDX spectra of the intermediates collected at different reaction times: (a) 2 h; (b) 3 h; (c) 4 h; (d) 5 h. It was found that the S component decreased and disappeared after 5h, while the P component increased with the elongation of the reaction time. The results indicate that more and more hybrid precursors were converted into FeP along with the reaction time increasing.

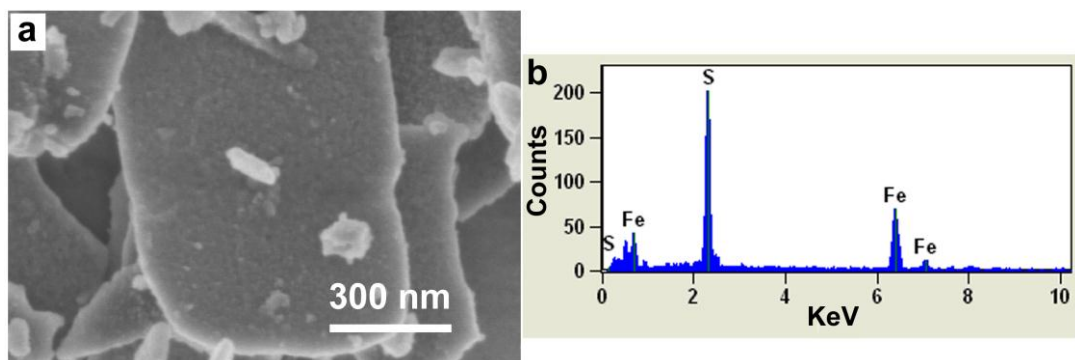


**Fig. S8** (a) SEM image and (b) EDX spectrum of the products when TOP was not introduced into the transformation process while other conditions were unchanged. It was found that TETAH molecules were extracted from  $\text{Fe}_{18}\text{S}_{25}$ -TETAH nanosheets, resulting in the in-situ formation of iron sulphide nanosheets with rough surface. These results suggest that the dissolution of TETAH molecules in 1-octadecene solution is helpful for the appearance of pores. Note more study should be done to characterize their crystal structure and to test their applications. These studies will be done in our later work.

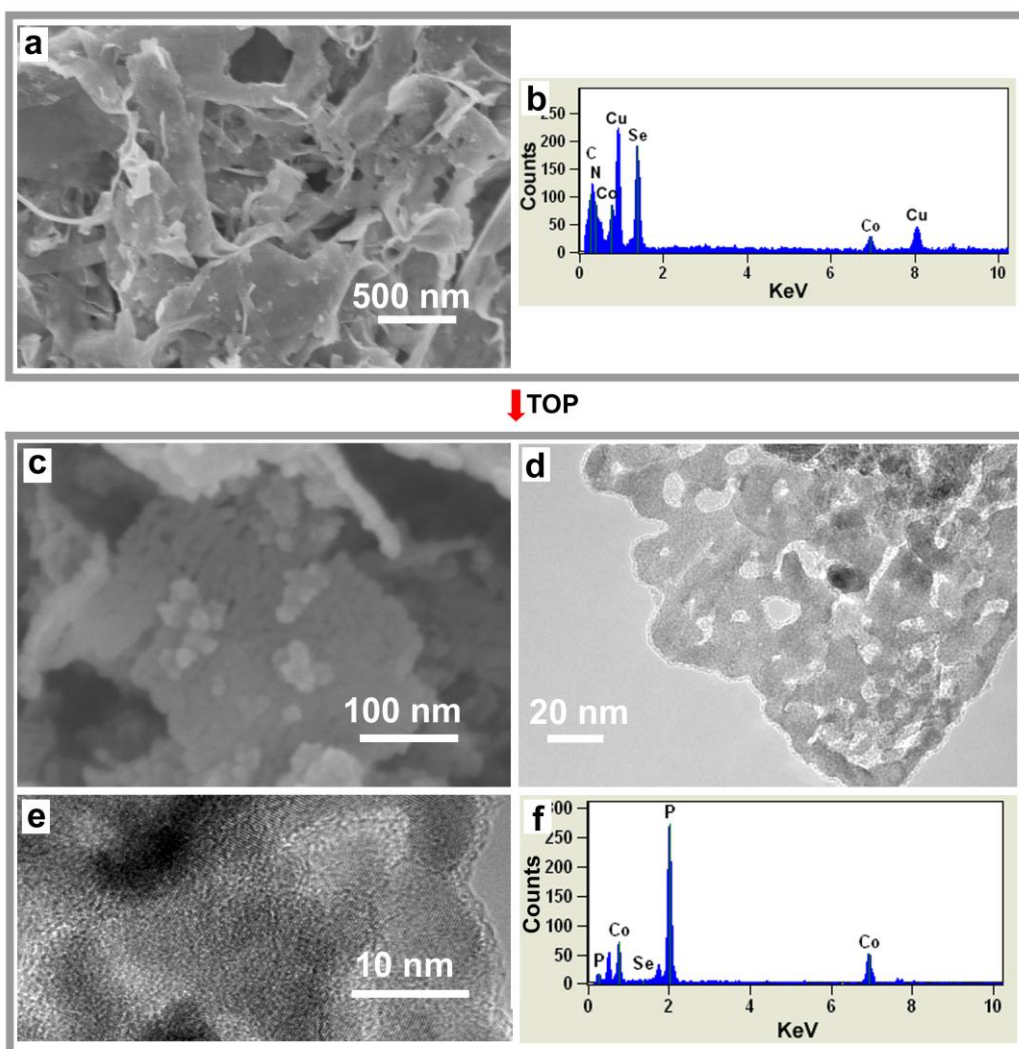


**Fig. S9** (a) SEM image and (b) EDX spectrum of the inorganic-organic hybrid  $\text{CoSe}_2$ -DETA nanosheets. (c) SEM image, (d) TEM image, (e) HRTEM image and (f) EDX spectrum of the porous cobalt phosphide nanosheets. In the EDX spectrum, the detected Cu singles arise from the Cu foil on which the samples were deposited. It can be seen that porous cobalt phosphide nanobelts were obtained after treating the inorganic-organic hybrid  $\text{CoSe}_2$ -DETA precursors with TOP. These results indicate that the anion-exchange strategy of hybrid precursors with TOP can be extended to the preparation of other porous nanostructures of transition metal phosphides.

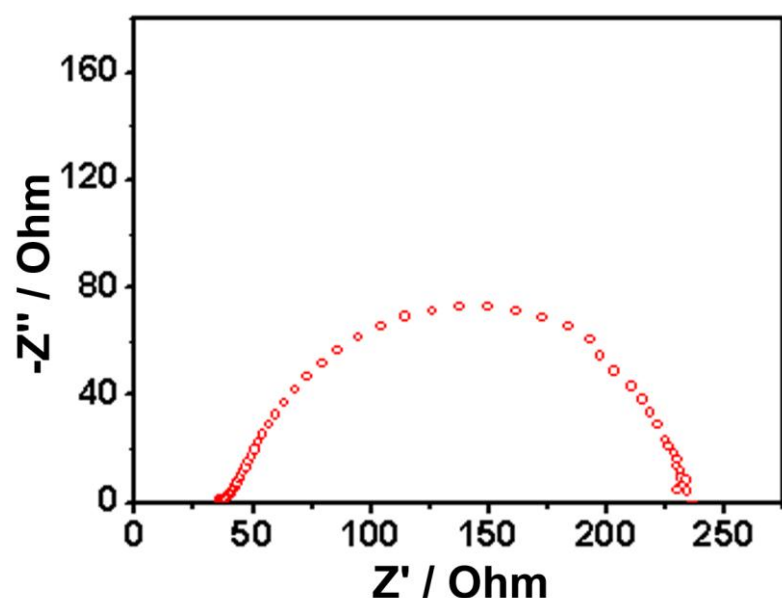


**Fig. S10** AC impedance spectroscopy study of porous FeP nanosheets at  $\eta = 0.14\text{V}$ . The result showed that porous FeP nanosheets exhibited small impedance (Faradic impedance, or charge-transfer impedance, of about  $200 \Omega$ ).